Finite-Horizon H_∞ Consensus Control for IoT-Enabled Multi-Agent Systems With Stochastic Scheduling and Relay-Assisted Communications

Jie Ban, Liangdong Guo, Zidong Wang, and Lei Zou

***Abstract*—The Internet of Things (IoT) increasingly relies on large-scale networked agents that cooperate over bandwidth-limited and unreliable wireless links. This paper studies the finite-horizon H_∞ consensus control problem for a class of discrete-time IoT-enabled multi-agent systems subject to random parameters, stochastic communication scheduling, and relay-assisted transmissions. To reflect practical IoT communication constraints, a novel transmission framework is considered that integrates a stochastic communication protocol with a decode-and-forward relay mechanism under random packet losses. Within this framework, only a subset of sensing information is scheduled for transmission, encoded, decoded, and forwarded by relay nodes to improve communication reliability and coverage. Based on the resulting networked system model, a distributed consensus controller is designed to attenuate the effects of disturbances and communication uncertainties over a finite time horizon. Sufficient conditions guaranteeing finite-horizon H_∞ consensus are derived in terms of recursive linear matrix inequalities, and a corresponding controller synthesis algorithm is developed. Simulation results illustrate the effectiveness of the proposed approach in achieving robust consensus for IoT-enabled multi-agent systems operating over stochastic relay-assisted communication networks.**

***Index Terms*—Multi-Agent systems; H_∞ consensus control; stochastic communication protocol; decode-and-forward relay; packet losses**

Abbreviations and Notations

$\mathbb{R}^{n\times m}$	The set of all $n \times m$ real matrices
$\mathbb{R}^n$	The set of all $n-$dimensional real vector
$R > 0$	The matrix R is positive definite
I	The identity matrix with an appropriate dimension
0	The zero matrix with an appropriate dimension
$*$	The symmetric part in the symmetric matrix
$\otimes$	The Kronecker product
$\text{sym}\{X\}$	The summation of X and its transpose X^T
Q^T	The transposition of the matrix Q
$\text{diag}\{\cdots\}$	The block-diagonal matrix
$\text{col}\{\cdots\}$	The column vector
$\mathbb{E}\{\cdot\}$	The expectation operator
$\lVert x\rVert$	The Euclidean norm of x

This work was supported in part by the National Natural Science Foundation of China under Grant 61773013, the Royal Society of the UK, and the Alexander von Humboldt Foundation of Germany. *(Corresponding author: Liangdong Guo).*

Jie Ban and Liangdong Guo are with the School of Electronic and Information Engineering, University of Science and Technology Liaoning, Anshan 114051, China (e-mails: banjie@ustl.edu.cn; ldguo@ustl.edu.cn).

Zidong Wang is with the Department of Computer Science, Brunel University of London, Uxbridge, Middlesex, UB8 3PH, United Kingdom (e-mail: Zidong.Wang@brunel.ac.uk).

Lei Zou is with the School of Information and Intelligent Science, Donghua University, Shanghai, China (e-mail: zouleicup@gmail.com).

I. Introduction

The Internet of Things (IoT) paradigm is enabling large-scale interconnected systems in which massive numbers of devices cooperate through wireless communication networks to accomplish complex tasks [1], [2]. In this context, multi-agent systems (MASs) have emerged as a fundamental modeling and control framework for IoT-enabled applications, owing to their inherent scalability, distributed decision-making capability, and adaptability to dynamic environments [3]–[5]. In an IoT-enabled MAS, each agent is typically equipped with sensing, computation, and communication modules, allowing it to perceive local environmental states, exchange information with neighboring agents, and execute coordinated control actions to achieve global objectives [6], [7]. Representative applications include drone swarms, cooperative mobile robots, autonomous driving systems, and satellite constellations, all of which rely on reliable information exchange and coordinated control over wireless networks [8]–[11].

Among various coordination tasks in IoT-enabled MASs, consensus control plays a central role, as it provides a fundamental mechanism for achieving agreement among distributed agents through local interactions. Over the past decade, significant progress has been made in consensus control for MASs, including adaptive and learning-based strategies for nonlinear systems [12], human-in-the-loop coordination under external disturbances [13], and optimization-oriented consensus with time delays [14]–[17]. However, most existing works assume that system parameters are time-invariant, which may not be realistic in IoT environments where operating conditions are highly dynamic [18]–[20].

In practical IoT deployments, agent dynamics often exhibit time-varying characteristics due to factors such as component aging, environmental variations, and changing workloads. This has motivated increasing research interest in time-varying MASs. For example, distributed H_∞ consensus control has been studied for discrete-time MASs with random parameters using recursive linear matrix inequalities (RLMIs) [21], while prescribed-time consensus strategies have been developed for time-varying systems with communication delays [22]. These studies provide valuable insights, yet they typically overlook communication constraints that are intrinsic to IoT networks.

In large-scale IoT systems, wireless communication resources are inherently limited. Bandwidth constraints, interference, and shared communication channels may lead to data collisions and packet losses, which can significantly degrade closed-loop performance [23], [24]. To address these challenges, various communication scheduling protocols have been introduced, including round-robin protocols [25], [26], try-once-discard protocols [27], [28], and stochastic communication protocols (SCPs) [29], [30]. Among them, SCPs are particularly attractive for IoT applications due to their low implementation complexity and strong robustness against interference. Recent works have demonstrated the effectiveness of SCPs in state estimation and control under unreliable communication conditions [31], [32].

Beyond scheduling, long-distance wireless transmission in IoT networks is often affected by path loss, multipath fading, and noise, especially in scenarios involving sparse infrastructure or wide-area deployments [33], [34]. Cooperative relay communication has been widely recognized as an effective means to enhance transmission reliability and coverage [35]–[37]. Depending on the processing strategy, relays can be classified into amplify-and-forward, decode-and-forward (DaF), and filter-and-forward types [38]–[41]. Among these, DaF relays are particularly suitable for IoT applications, as they improve transmission quality through encoding and decoding operations while also enhancing data confidentiality. As a result, DaF-based relay mechanisms have attracted growing attention in recent years [42]–[44].

In the context of encoding and decoding mechanisms, in [45], [46], the problem of recursive state estimation has been addressed for networked systems operating over relay channels. Specifically, [45] has investigated the finite-horizon state estimation problem for a class of nonlinear time-varying complex dynamical networks with stochastic coupling, where a relay-based strategy employing the DaF protocol has been introduced to schedule data transmission from sensors to the remote estimator in order to ensure communication quality. In [46], to further preserve data privacy during the relaying process, a decryption-free relaying protocol has been developed, and a matrix-inequality-based approach has been proposed for parameter design. Quantization effects have been widely studied in networked control systems due to their close connection with bandwidth-limited communication. Prior works [47], [48] have investigated mismatched quantized H_∞ output-feedback control for fuzzy Markov jump systems and robust H_2 control of linear systems to mitigate performance degradation caused by inconsistent quantization across system components. To the best of our knowledge, the finite-horizon H_∞ consensus control problem for IoT-enabled multi-agent systems based on SCP and DaF protocols has not yet been investigated in the existing literature, and the objective of this paper is therefore to address this research gap.

Motivated by the above observations, this paper investigates the finite-horizon H_∞ consensus control problem for a class of discrete-time multi-agent systems with random parameters operating over IoT-style wireless networks. A transmission framework that integrates SCP-based scheduling with DaF relay-assisted communication is considered. This problem remains unexplored in the current literature and presents significant challenges due to the following difficulties: 1) how to design an efficient DaF relay framework for discrete-time multi-agent systems with random parameters? 2) how to accurately evaluate the H_∞ consensus performance of multi-agent systems affected by data loss, random parameters, and SCP? 3) how to design controller gains to guarantee the H_∞ performance constraint? To address these issues, the main contributions of this paper are summarized as follows.

1) The finite-horizon H_∞ control problem for MASs with random variables under the combined effects of SCP and the DaF relay protocol is studied for the first time. The proposed H_∞ control framework integrates random scheduling constraints, encoding-decoding mechanisms, and packet loss effects arising from relay communication.
2) A cooperative control framework is developed to handle the compounded challenges introduced by SCP and DaF protocols. Simultaneous improvements in communication quality and transmission range are achieved, while the encoding-decoding mechanism ensures data security.
3) For discrete-time MASs with random variables, a novel finite-horizon H_∞ consensus control framework based on SCP-DaF is proposed. Sufficient conditions for satisfying the H_∞ performance constraint are established in terms of RLMIs, and an algorithm based on SCP-DaF is developed to compute the control gain matrix.

The subsequent sections are organized as follows. In Section II, the SCP and DaF relay strategies are introduced, and a controller based on SCP and DaF is designed. Based on this, a model transformation is performed, and the final finite-horizon H_∞ consensus control constraints are derived. Section III presents the main theoretical results, where sufficient conditions are derived to guarantee that the stochastic MASs achieve finite-horizon H_∞ consensus. Moreover, an algorithm is proposed for computing the controller gain matrix. In Section IV, a numerical simulation example is provided to validate the effectiveness of the proposed method, and the results are analyzed and discussed. Finally, conclusions and directions for future research are given in Section V.

II. Problem Formulation and Preliminaries

A. Graph Theory and System Model

In this paper, a discrete-time MAS with random variables is considered, consisting of J agents with the communication topology represented by a directed graph $\mathcal{G} \triangleq (\mathcal{J}, \mathcal{N}, \mathcal{A})$, where $\mathcal{J} \triangleq \{1, 2, \dots, J\}$ denotes the set of agents, $\mathcal{N} \triangleq \mathcal{J} \times \mathcal{J}$ is the set of edges, and $\mathcal{A} \triangleq [a_{lk}]$ with $a_{lk} > 0$ represents the weighted adjacency matrix. A directed edge $(l, k) \in \mathcal{N}$ denotes the information of agent j can be received by agent i. For the elements of $\mathcal{A}$, $a_{lk} = 1$ indicates that $(l, k) \in \mathcal{N}$, whereas $a_{lk} = 0$ implies $(l, k) \notin \mathcal{N}$. Additionally, self-edges (l, l) are excluded for any $l \in \mathcal{J}$. The Laplacian matrix is defined as $\mathcal{L} \triangleq \mathcal{A} - \mathcal{D}$, where $\mathcal{D} \triangleq \text{diag}\{d_1, d_2, \dots, d_J\}$, $d_l \triangleq \sum_{k \in \mathcal{J}_l} a_{lk}$, $\mathcal{J}_l$ denotes the neighbor set of node l.

Consider a class of discrete-time MASs consisting of $\mathcal{J}$ agents with random variables. The dynamics of the l-th agent are modeled as follows:

$$\begin{cases} x_l(s+1) = \big(A(s)+G(s)\mu(s)\big)x_l(s)+B(s)u_l(s) \\ \qquad\qquad +C(s)\omega_l(s) \\ y_l(s) = D(s)x_l(s)+E(s)v_l(s) \\ z_l(s) = F(s)x_l(s) \end{cases} \tag{1}$$

where $x_l(s)\in\mathbb{R}^{n_x}$, $y_l(s)\in\mathbb{R}^{n_y}$, $z_l(s)\in\mathbb{R}^{n_z}$, and $u_l(s)\in\mathbb{R}^{n_u}$ are, respectively, denote the system state, measured output vector, control output, and the required control input of the l-th agent; $A(s)$, $B(s)$, $C(s)$, $D(s)$, $E(s)$, $F(s)$ and $G(s)$ are known time-varying matrices with appropriate dimensions; $\omega_l(s)\in\mathcal{L}_\infty^{n_v}$ and $v_l(s)\in\mathcal{L}_\infty^{n_v}$ represent the exogenous disturbances; $\mu(s)\in\mathbb{R}$ denotes a one-dimensional Gaussian white noise sequence. For notational convenience, the measurement output vector is defined as $y_l(s)=\mathrm{col}\{y_{l1},y_{l2},\ldots,y_{ln_y}\}$.

B. SCP Protocol

During data transmission, bandwidth constraints may lead to data collisions. To address this issue, the SCP protocol is employed in this paper to coordinate data exchange, effectively preventing conflicts and enhancing transmission efficiency. Under the SCP scheduling protocol, each agent l is constrained to transmit exactly one datum per time slot s. As established in [49], the SCP can be characterized as a stochastic process, where $\gamma(s)$ denotes the permission marker for data transmission through the communication channel at time s. Given $\Upsilon\triangleq\{1,2,\ldots,n_y\}$, the probability that $\gamma(s+1)=m$ given $\gamma(s)=t$ is characterized by

$$\mathbf{P}\{\gamma(s+1)=m|\gamma(s)=t\}=p_{tm}, t,m\in\Upsilon$$

where $p_{tm}\geq 0$, $\sum_{m=1}^{n_y}p_{tm}=1$. The transition probability matrix and the updating matrix are denoted by $\mathrm{P}\triangleq[p_{tm}]_{n_y\times n_y}$ and $\Psi_{\gamma(s)}\triangleq\mathrm{diag}\{\delta(1,\gamma(\mathrm{s})),\delta(2,\gamma(\mathrm{s})),\ldots,\delta(\mathrm{n_y},\gamma(\mathrm{s}))\}$, respectively, where $\delta(\cdot)$ represents the Kronecker delta function. Accordingly, the measurement output after SCP scheduling is modeled as

$$\hat{y}_l(s)=\Psi_{\gamma(s)}y_l(s). \tag{2}$$

C. DaF Relay Protocol

The output signal, after being scheduled by the SCP, will be transmitted through the communication channel to the next stage. During this process, the signal passes through a relay-based communication network before finally reaching the controller. This paper proposes an encode-decode-forward mechanism within the communication link to extend the data transmission range and enhance communication efficiency.

1) Encoding Procedure: During this process, the SCP-scheduled output signal $\hat{y}_l(s)$ is encoded as:

$$g_l(s)=\mathfrak{E}_l(\hat{y}_l(s))=\xi_l(q_l(\hat{y}_l(s))) \tag{3}$$

where $\xi_l(q_l(\hat{y}_l(s)))\triangleq\mathrm{col}\big\{\xi_{l1}(q_{l1}(\hat{y}_{l1}(s))),\xi_{l2}(q_{l2}(\hat{y}_{l2}(s))),\ldots,\xi_{ln_y}(q_{ln_y}(\hat{y}_{ln_y}(s)))\big\}$, and $q_{lj}(\hat{y}_{lj}(s))$ is a scalar quantizer defined as:

$$q_{lj}(\hat{y}_{lj}(s))=\begin{cases} -c_{lj}, & \hat{y}_{lj}(s)\leq -c_{lj} \\ \underline{c}_{lj}, & \underline{c}_{lj}\leq\hat{y}_{lj}(s)<\bar{c}_{lj} \\ c_{lj}, & \hat{y}_{lj}(s)\geq c_{lj} \end{cases} \tag{4}$$

here, c_{lj} denotes the given amplitude value, with the quantization parameters determined by a positive constant b that specifies the number of equal divisions over $[-c_{lj},c_{lj}]$. The lower and upper bounds of the e-th subinterval are respectively given by:

$$\underline{c}_{lj}=\frac{(2e-1)c_{lj}}{b}-c_{lj},\quad \bar{c}_{lj}=\frac{2ec_{lj}}{b}-c_{lj}.$$

It is essential to note that the function $\xi_{lj}(\cdot)$ is an index generator function and satisfies

$$\xi_{lj}(q_{lj}(\hat{y}_{lj}(s)))\in\{1,2,\ldots,b\}.$$

Let $\nu_{lj}(s)\triangleq q_{lj}(\hat{y}_{lj}(s))-\hat{y}_{lj}(s)$ denote the encode error, which is bounded by: $\|\nu_{lj}(s)\|\leq\frac{c_{lj}}{b}$.

2) Decoding and Forwarding Procedure: In this process, the encoded data will be decoded prior to transmission, and the decoded signal with the packet dropout phenomenon can be expressed as:

$$d_l(s)=\alpha_l(s)\mathfrak{D}_l\big(g_l(s)\big) \tag{5}$$

where

$$\mathfrak{D}_l\big(g_l(s)\big)\triangleq\mathrm{col}\Big\{\mathfrak{D}_{l1}\big(g_{l1}(s)\big),\mathfrak{D}_{l2}\big(g_{l2}(s)\big),\ldots,\mathfrak{D}_{ln_y}\big(g_{ln_y}(s)\big)\Big\}.$$

The mapping $\mathfrak{D}_l\big(g_l(s)\big)$ decodes the encoded signal $g_l(s)$ into the output signal $\hat{y}_l(s)$, which can be further specified as:

$$\mathfrak{D}_{lj}\big(g_{lj}(s)\big)=\frac{\big(2g_{lj}(s)-1\big)c_{lj}}{b}-c_{lj}.$$

Then, denoting $\vartheta_{lj}(s)\triangleq\mathfrak{D}_{lj}\big(g_{lj}(s)\big)-\hat{y}_{lj}(s)$ as the decode error, it is easily obtained that $\nu_{lj}(s)=\vartheta_{lj}(s)$, and we can finally derive the decoded signal as

$$d_l(s)=\alpha_l(s)\big(\hat{y}_l(s)+\nu_l(s)\big) \tag{6}$$

where $\nu_l(s)\triangleq\mathrm{col}\{\nu_{l1}(s),\nu_{l2}(s),\ldots,\nu_{ln_y}(s)\}$, $\alpha_l(s)$ is a Bernoulli-distributed random variable that characterizes packet loss and satisfies the following distribution:

$$\mathbf{P}\{\alpha_l(s)=0\}=1-\bar{\alpha}_l,\quad \mathbf{P}\{\alpha_l(s)=1\}=\bar{\alpha}_l.$$

The decoded signal is then amplified and forwarded by the relay node, where packet loss is also considered. The signal transmitted by the relay node can be expressed as:

$$r_l(s)=\sqrt{W_l}\beta_l(s)d_l(s)+H_l(s)n_l(s) \tag{7}$$

where W_l denotes the average signal energy, $H_l(s)$ is a known matrix with appropriate dimensions, $n_l(s)\in l_2\big([0,T],\mathbb{R}^{n_l}\big)$ represents the noise vector within the finite-time horizon $[0,T]$. Moreover, the Bernoulli random variable $\beta_l(s)$, which characterizes the random packet loss phenomenon, follows the following Bernoulli distribution:

$$\mathbf{P}\{\beta_l(s)=0\}=1-\bar{\beta}_l,\quad \mathbf{P}\{\beta_l(s)=1\}=\bar{\beta}_l.$$

D. SCP-DaF-based Controller Design and Model Transformation

Within the communication framework integrating the SCP scheduling and the DaF relaying, the terminal measurement output $r_l(s)$ is transmitted to the remote controller via distributed multi-agent interactions. Then, by incorporating neighbor-agent information exchange to achieve cooperative control under stochastic communication constraints, a novel distributed controller is designed as follows:

$$u_l(s) = K_{\gamma(s)}(s) \sum_{k\in\mathcal{J}_l} a_{lk}\big(r_l(s) - r_k(s)\big) \tag{8}$$

where $K_{\gamma(s)}(s)$ is the gain matrix at time s, which needs to be designed.

To facilitate the subsequent analysis while ensuring clarity, we adopt the following notations:

$$\begin{aligned}
x(s) &\triangleq \mathrm{col}\{x_1(s), x_2(s), \dots, x_J(s)\}\\
y(s) &\triangleq \mathrm{col}\{y_1(s), y_2(s), \dots, y_J(s)\}\\
\omega(s) &\triangleq \mathrm{col}\{\omega_1(s), \omega_2(s), \dots, \omega_J(s)\}\\
v(s) &\triangleq \mathrm{col}\{v_1(s), v_2(s), \dots, v_J(s)\}\\
u(s) &\triangleq \mathrm{col}\{u_1(s), u_2(s), \dots, u_J(s)\}\\
z(s) &\triangleq \mathrm{col}\{z_1(s), z_2(s), \dots, z_J(s)\}\\
n(s) &\triangleq \mathrm{col}\{n_1(s), n_2(s), \dots, n_J(s)\}\\
\nu(s) &\triangleq \mathrm{col}\{\nu_1(s), \nu_2(s), \dots, \nu_J(s)\}.
\end{aligned}$$

By employing the Kronecker product, based on (2), (6), (7), (8) and the definition of $\nu_l(s)$, we obtain the following compact form of the stochastic MAS (1):

$$\begin{cases}
x(s+1) = \Big(I_J \otimes \big(A(s) + G(s)\mu(s)\big)\\
\qquad\qquad +\big(W\rho(s)\mathcal{L} \otimes B(s)K_{\gamma(s)}(s)\Psi_{\gamma(s)}D(s)\big)\Big)x(s)\\
\qquad\qquad +\Big(W\rho(s)\mathcal{L} \otimes B(s)K_{\gamma(s)}(s)\Psi_{\gamma(s)}E(s)\Big)v(s)\\
\qquad\qquad +\Big(W\rho(s)\mathcal{L} \otimes B(s)K_{\gamma(s)}(s)\Big)\nu(s)\\
\qquad\qquad +\big(H(s)\mathcal{L} \otimes B(s)K_{\gamma(s)}(s)\big)n(s)\\
\qquad\qquad +\big(I_J \otimes C(s)\big)\omega(s)\\
y(s) = \big(I_J \otimes D(s)\big)x(s) + (I_J \otimes E(s))v(s)\\
z(s) = \big(I_J \otimes F(s)\big)x(s)
\end{cases} \tag{9}$$

where

$$\begin{aligned}
&W \triangleq \mathrm{diag}\{\sqrt{W_1}, \sqrt{W_2}, \dots, \sqrt{W_J}\}\\
&\rho(s) \triangleq \mathrm{diag}\{\alpha_1(s)\beta_1(s), \alpha_2(s)\beta_2(s), \dots, \alpha_J(s)\beta_J(s)\}\\
&H(s) \triangleq \mathrm{diag}\{H_1(s), H_2(s), \dots, H_J(s)\}.
\end{aligned}$$

Define the deviations of the state vector $x_l(s)$ and the controlled output $z_l(s)$ for the l-th agent relative to the mean values across all J agents:

$$\begin{aligned}
\bar{x}_l(s) &\triangleq x_l(s) - \frac{1}{J}\sum_{l=1}^{J} x_l(s)\\
\bar{z}_l(s) &\triangleq z_l(s) - \frac{1}{J}\sum_{l=1}^{J} z_l(s).
\end{aligned}$$

Then, one can easily derive that

$$\begin{cases}
\bar{x}(s+1) = \Big(I_J \otimes \big(A(s) + G(s)\mu(s)\big)\\
\qquad\qquad +\big(W\rho(s)\mathcal{L} \otimes B(s)K_{\gamma(s)}(s)\Psi_{\gamma(s)}D(s)\big)\Big)\bar{x}(s)\\
\qquad\qquad +\Big(W\rho(s)\mathcal{J}\mathcal{L} \otimes B(s)K_{\gamma(s)}(s)\Psi_{\gamma(s)}E(s)\Big)v(s)\\
\qquad\qquad +\Big(W\rho(s)\mathcal{J}\mathcal{L} \otimes B(s)K_{\gamma(s)}(s)\Big)\nu(s)\\
\qquad\qquad +\big(H(s)\mathcal{J}\mathcal{L} \otimes B(s)K_{\gamma(s)}(s)\big)n(s)\\
\qquad\qquad +\big(\mathcal{J} \otimes C(s)\big)\omega(s)\\
\bar{z}(s) = \big(I_J \otimes F(s)\big)\bar{x}(s)
\end{cases} \tag{10}$$

where $\mathcal{J} \triangleq \begin{bmatrix} \frac{J-1}{J} & -\frac{1}{J} & \cdots & -\frac{1}{J}\\ -\frac{1}{J} & \frac{J-1}{J} & \cdots & -\frac{1}{J}\\ \vdots & \vdots & \ddots & \vdots\\ -\frac{1}{J} & -\frac{1}{J} & \cdots & \frac{J-1}{J} \end{bmatrix}$.

From the definition of $\mathcal{J}$, the following result holds directly:

$$\mathcal{J}\mathcal{L} = \mathcal{L}. \tag{11}$$

Defining $\chi(s) \triangleq \mathrm{col}\{x(s), \bar{x}(s)\}$ and combining (9)-(11), we obtain the augmented system as:

$$\begin{cases}
\chi(s+1) = \big(\mathfrak{A}(s) + \mathfrak{G}_{\gamma(s)}(s)\big)\chi(s) + \mathfrak{B}_{\gamma(s)}(s)v(s)\\
\qquad\qquad +\mathfrak{C}(s)\omega(s) + \mathfrak{E}_{\gamma(s)}(s)\nu(s) + \mathfrak{D}_{\gamma(s)}(s)n(s)\\
\bar{z}(s) = \mathfrak{F}(s)\chi(s)
\end{cases} \tag{12}$$

where

$$\begin{aligned}
&\mathfrak{A}(s) \triangleq \mathfrak{A}_1(s) + \mathfrak{A}_2(s), \quad \mathfrak{F}(s) \triangleq \begin{bmatrix} 0 & I_J \otimes F(s) \end{bmatrix}\\
&\mathfrak{A}_1(s) \triangleq \begin{bmatrix} I_J \otimes A(s) & 0\\ 0 & I_J \otimes A(s)) \end{bmatrix}\\
&\mathfrak{A}_2(s) \triangleq \begin{bmatrix} I_J \otimes G(s)\mu(s) & 0\\ 0 & I_J \otimes G(s)\mu(s) \end{bmatrix}\\
&\mathfrak{G}_{\gamma(s)}(s) \triangleq \begin{bmatrix} \mathfrak{G}^{11}_{\gamma(s)}(s) & 0\\ 0 & \mathfrak{G}^{22}_{\gamma(s)}(s) \end{bmatrix}, \quad \mathfrak{C}(s) \triangleq \begin{bmatrix} I_J \otimes C(s)\\ \mathcal{J} \otimes C(s) \end{bmatrix}\\
&\mathfrak{G}^{11}_{\gamma(s)}(s) \triangleq W\rho(s)\mathcal{L} \otimes B(s)K_{\gamma(s)}(s)\Psi_{\gamma(s)}D(s)\\
&\mathfrak{G}^{22}_{\gamma(s)}(s) \triangleq W\rho(s)\mathcal{J}\mathcal{L} \otimes B(s)K_{\gamma(s)}(s)\Psi_{\gamma(s)}D(s)\\
&\mathfrak{B}_{\gamma(s)}(s) \triangleq \begin{bmatrix} W\rho(s)\mathcal{L} \otimes B(s)K_{\gamma(s)}(s)\Psi_{\gamma(s)}E(s)\\ W\rho(s)\mathcal{J}\mathcal{L} \otimes B(s)K_{\gamma(s)}(s)\Psi_{\gamma(s)}E(s) \end{bmatrix}\\
&\mathfrak{E}_{\gamma(s)}(s) \triangleq \begin{bmatrix} W\rho(s)\mathcal{L} \otimes B(s)K_{\gamma(s)}(s)\\ W\rho(s)\mathcal{J}\mathcal{L} \otimes B(s)K_{\gamma(s)}(s) \end{bmatrix}\\
&\mathfrak{D}_{\gamma(s)}(s) \triangleq \begin{bmatrix} H(s)\mathcal{L} \otimes B(s)K_{\gamma(s)}(s)\\ H(s)\mathcal{J}\mathcal{L} \otimes B(s)K_{\gamma(s)}(s) \end{bmatrix}.
\end{aligned}$$

Letting $\tilde{\rho}(s) \triangleq \rho(s) - \bar{\rho}$, the augmented system (12) can be reformulated as:

$$\begin{cases}
\chi(s+1) = \big(\mathfrak{A}(s) + \tilde{\mathfrak{G}}_{\gamma(s)}(s) + \bar{\mathfrak{G}}_{\gamma(s)}(s)\big)\chi(s)\\
\qquad\qquad +\big(\tilde{\mathfrak{B}}_{\gamma(s)}(s) + \bar{\mathfrak{B}}_{\gamma(s)}(s)\big)v(s)\\
\qquad\qquad +\big(\tilde{\mathfrak{E}}_{\gamma(s)}(s) + \bar{\mathfrak{E}}_{\gamma(s)}(s)\big)\nu(s)\\
\qquad\qquad +\mathfrak{D}_{\gamma(s)}(s)n(s) + \mathfrak{C}(s)\omega(s)\\
\bar{z}(s) = \mathfrak{F}(s)\chi(s)
\end{cases} \tag{13}$$

where

$$\begin{aligned}
&\bar{\rho} \triangleq \mathrm{diag}\{\bar{\rho}_1, \bar{\rho}_2, \dots, \bar{\rho}_J\}, \quad \bar{\rho}_l \triangleq \bar{\alpha}_l\bar{\beta}_l\\
&\bar{\mathfrak{G}}_{\gamma(s)}(s) \triangleq \begin{bmatrix} \bar{\mathfrak{G}}^{11}_{\gamma(s)}(s) & 0\\ 0 & \bar{\mathfrak{G}}^{22}_{\gamma(s)}(s) \end{bmatrix}
\end{aligned}$$

$$\bar{\mathfrak{G}}^{11}_{\gamma(s)}(s) \triangleq W\bar{\rho}\mathcal{L} \otimes B(s)K_{\gamma(s)}(s)\Psi_{\gamma(s)}D(s)$$
$$\bar{\mathfrak{G}}^{22}_{\gamma(s)}(s) \triangleq W\bar{\rho}\mathcal{J}\mathcal{L} \otimes B(s)K_{\gamma(s)}(s)\Psi_{\gamma(s)}D(s)$$
$$\tilde{\mathfrak{G}}_{\gamma(s)}(s) \triangleq \begin{bmatrix} \tilde{\mathfrak{G}}^{11}_{\gamma(s)}(s) & 0 \\ 0 & \tilde{\mathfrak{G}}^{22}_{\gamma(s)}(s) \end{bmatrix}$$
$$\tilde{\mathfrak{G}}^{11}_{\gamma(s)}(s) \triangleq W\tilde{\rho}(s)\mathcal{L} \otimes B(s)K_{\gamma(s)}(s)\Psi_{\gamma(s)}D(s)$$
$$\tilde{\mathfrak{G}}^{22}_{\gamma(s)}(s) \triangleq W\tilde{\rho}(s)\mathcal{J}\mathcal{L} \otimes B(s)K_{\gamma(s)}(s)\Psi_{\gamma(s)}D(s)$$
$$\bar{\mathfrak{B}}_{\gamma(s)}(s) \triangleq \begin{bmatrix} W\bar{\rho}\mathcal{L} \otimes B(s)K_{\gamma(s)}(s)\Psi_{\gamma(s)}E(s) \\ W\bar{\rho}\mathcal{J}\mathcal{L} \otimes B(s)K_{\gamma(s)}(s)\Psi_{\gamma(s)}E(s) \end{bmatrix}$$
$$\tilde{\mathfrak{B}}_{\gamma(s)}(s) \triangleq \begin{bmatrix} W\tilde{\rho}(s)\mathcal{L} \otimes B(s)K_{\gamma(s)}(s)\Psi_{\gamma(s)}E(s) \\ W\tilde{\rho}(s)\mathcal{J}\mathcal{L} \otimes B(s)K_{\gamma(s)}(s)\Psi_{\gamma(s)}E(s) \end{bmatrix}$$
$$\bar{\mathfrak{E}}_{\gamma(s)}(s) \triangleq \begin{bmatrix} W\bar{\rho}\mathcal{L} \otimes B(s)K_{\gamma(s)}(s) \\ W\bar{\rho}\mathcal{J}\mathcal{L} \otimes B(s)K_{\gamma(s)}(s) \end{bmatrix}$$
$$\tilde{\mathfrak{E}}_{\gamma(s)}(s) \triangleq \begin{bmatrix} W\tilde{\rho}(s)\mathcal{L} \otimes B(s)K_{\gamma(s)}(s) \\ W\tilde{\rho}(s)\mathcal{J}\mathcal{L} \otimes B(s)K_{\gamma(s)}(s) \end{bmatrix}.$$

As analyzed, the augmented system (13) is subject to random parameters and external disturbances. The objective of this paper is to design an effective controller gain $K_{\gamma(s)}(s)$ such that system (13) achieves the H_∞ performance requirement. To this end, the following finite-horizon H_∞ consensus constraints are proposed.

Definition 1: For a given directed graph $\mathcal{G}$, disturbance attenuation level $\lambda > 0$, and positive definite symmetric matrix Π, the SCP-DaF-based augmented system (13) is said to achieve finite-horizon H_∞ consensus if the following inequality holds over the finite time horizon $[0, \mathcal{S}-1]$:

$$\mathbb{E}\Big\{\sum_{s=0}^{\mathcal{S}-1}\Big(\|\bar{z}(s)\|^2 - \lambda^2\big(\|v(s)\|^2 + \|\omega(s)\|^2 + \|n(s)\|^2 + \tilde{c}\big)\Big) - \lambda^2\chi^T(0)(I_J \otimes \Pi)\chi(0)\Big\} < 0 \tag{14}$$

where $\tilde{c} \triangleq \sum_{l=1}^{J}\sum_{j=1}^{n_y}(\frac{c_{lj}}{b})^2$.

Remark 1: In this paper, the SCP is integrated with the DaF relay strategy. After being output from the sensor, the signal is first scheduled by the SCP, ensuring that only one output component is transmitted. Before the signal is received by the relay, encoding-decoding processing is applied to ensure information security and reliability. The model explicitly incorporates random packet loss phenomena, quantified by Bernoulli-distributed random variables $\alpha_l(s)$ and $\beta_l(s)$, to account for practical communication impairments such as network-induced packet drops. Crucially, the synergistic implementation of SCP and DaF strategies introduces heightened complexity in signal handling, while the probabilistic packet loss characterization enhances the model's applicability to real-world engineering scenarios.

Remark 2: Unlike the related work in [45], Definition 1 provides an H_∞ performance index for a coupled augmented system model that simultaneously accounts for the random switching induced by SCP and the packet loss occurring during the DaF process. This study aims to design an appropriate controller gain $K_{\gamma(s)}(s)$ such that the augmented system (13) satisfies the finite-horizon H_∞ consensus condition defined in (14). It is particularly noteworthy that system (13) must account for random packet losses occurring in both the SCP scheduling and DaF relaying processes. This characteristic endows the system with superior efficiency and security in signal transmission compared to existing approaches.

III. Main Result

In this section, sufficient conditions are first established in the form of a theorem for the augmented system (13) to achieve finite-horizon H_∞ consensus over the time horizon $[0, \mathcal{S}-1]$, under the assumption that the gain matrix $K_{\gamma(s)}(s)$ is known. Building upon these results, solvability conditions for $K_{\gamma(s)}(s)$ are subsequently derived in terms of RLMIs. Without loss of clarity, $\gamma(s) \triangleq t$ is hereafter adopted for notational simplicity.

A. Finite-Horizon H_∞ Performance Analysis

Theorem 1: For any $t \in \Upsilon$, let a directed graph $\mathcal{G}$, disturbance attenuation level $\lambda > 0$ (i.e., the upper bound of the H_∞ consensus performance), positive definite symmetric matrix Π and controller gains be given. The stochastic system (13) satisfies the H_∞ consensus constrains (14) if there exists a set of non-negative definite matrices $\{Q_t(s)\}_{s\in\mathcal{S}-1}$ and the weighted sum $\bar{Q}_t(s) = \sum_{m=1}^{n_y} p_{tm}Q_m(s)$ ($t, m \in \Upsilon$ with $\bar{Q}_t(0) \le \lambda^2\Pi$) such that the following RLMI holds:

$$\Xi_t(s) = \begin{bmatrix} \Xi^t_{11}(s) & \Xi^t_{12}(s) & \Xi^t_{13}(s) & \Xi^t_{14}(s) & \Xi^t_{15}(s) \\ * & \Xi^t_{22}(s) & \Xi^t_{23}(s) & \Xi^t_{24}(s) & \Xi^t_{25}(s) \\ * & * & \Xi^t_{33}(s) & \Xi^t_{34}(s) & \Xi^t_{35}(s) \\ * & * & * & \Xi^t_{44}(s) & \Xi^t_{45}(s) \\ * & * & * & * & \Xi^t_{55}(s) \end{bmatrix} < 0 \tag{15}$$

where

$$\Xi^t_{11}(s) \triangleq \big(\mathfrak{A}_1(s) + \bar{\mathfrak{G}}_t(s)\big)^T\bar{Q}_t(s+1)\big(\mathfrak{A}_1(s) + \bar{\mathfrak{G}}_t(s)\big) + \Omega_1(s) - Q_t(s) + \mathfrak{F}^T(s)\mathfrak{F}(s) + \bar{\mathfrak{A}}^T_2(s)\bar{Q}_t(s+1) \times \bar{\mathfrak{A}}_2(s), \quad \bar{\mathfrak{A}}_2(s) \triangleq \begin{bmatrix} I_J \otimes G(s) & 0 \\ 0 & I_J \otimes G(s) \end{bmatrix}$$
$$\Xi^t_{12}(s) \triangleq \big(\mathfrak{A}(s) + \bar{\mathfrak{G}}_t(s)\big)^T\bar{Q}_t(s+1)\mathfrak{C}(s)$$
$$\Xi^t_{13}(s) \triangleq \big(\mathfrak{A}(s) + \bar{\mathfrak{G}}_t(s)\big)^T\bar{Q}_t(s+1)\bar{\mathfrak{B}}_t(s) + \Omega_2(s)$$
$$\Xi^t_{14}(s) \triangleq \big(\mathfrak{A}(s) + \bar{\mathfrak{G}}_t(s)\big)^T\bar{Q}_t(s+1)\bar{\mathfrak{E}}_t(s) + \Omega_3(s)$$
$$\Xi^t_{15}(s) \triangleq \big(\mathfrak{A}(s) + \bar{\mathfrak{G}}_t(s)\big)^T\bar{Q}_t(s+1)\mathfrak{D}(s)$$
$$\Xi^t_{22}(s) \triangleq \mathfrak{C}^T(s)\bar{Q}_t(s+1)\mathfrak{C}(s) - \lambda^2 I$$
$$\Xi^t_{23}(s) \triangleq \mathfrak{C}^T(s)\bar{Q}_t(s+1)\bar{\mathfrak{B}}_t(s)$$
$$\Xi^t_{24}(s) \triangleq \mathfrak{C}^T(s)\bar{Q}_t(s+1)\bar{\mathfrak{E}}_t(s)$$
$$\Xi^t_{25}(s) \triangleq \mathfrak{C}^T(s)\bar{Q}_t(s+1)\mathfrak{D}(s)$$
$$\Xi^t_{33}(s) \triangleq \bar{\mathfrak{B}}^T_t(s)\bar{Q}_t(s+1)\bar{\mathfrak{B}}_t(s) + \Omega_4(s) - \lambda^2 I$$
$$\Xi^t_{34}(s) \triangleq \bar{\mathfrak{B}}^T_t(s)\bar{Q}_t(s+1)\bar{\mathfrak{E}}_t(s) + \Omega_5(s)$$
$$\Xi^t_{35}(s) \triangleq \bar{\mathfrak{B}}^T_t(s)\bar{Q}_t(s+1)\mathfrak{D}(s)$$
$$\Xi^t_{45} \triangleq \bar{\mathfrak{E}}^T_t(s)\bar{Q}_t(s+1)\mathfrak{D}(s)$$
$$\Xi^t_{44}(s) \triangleq \bar{\mathfrak{E}}^T_t(s)\bar{Q}_t(s+1)\bar{\mathfrak{E}}_t(s) + \Omega_6(s) - \lambda^2 I$$
$$\Xi^t_{55}(s) \triangleq \mathfrak{D}^T(s)\bar{Q}_t(s+1)\mathfrak{D}(s) - \lambda^2 I$$
$$\Omega_1(s) \triangleq \sum_{l=1}^{J}\bar{\rho}_l\big(1 - \bar{\rho}_l\big)\tilde{\mathfrak{G}}^T_{t,l}(s)\bar{Q}_t(s+1)\tilde{\mathfrak{G}}_{t,l}(s)$$

$$
\begin{aligned}
&\tilde{\mathfrak{G}}_{t,l}(s) \triangleq \begin{bmatrix} \tilde{\mathfrak{G}}^{11}_{t,l}(s) & 0 \\ 0 & \tilde{\mathfrak{G}}^{22}_{t,l}(s) \end{bmatrix} \\
&\tilde{\mathfrak{G}}^{11}_{t,l}(s) \triangleq WI_l\mathscr{L} \otimes B(s)K_{\gamma(s)}(s)\Psi_{\gamma(s)}D(s) \\
&\tilde{\mathfrak{G}}^{22}_{t,l}(s) \triangleq WI_l\mathscr{G}\mathscr{L} \otimes B(s)K_{\gamma(s)}(s)\Psi_{\gamma(s)}D(s) \\
&I_l \triangleq \mathrm{diag}\{\underbrace{0,\ldots,0}_{l-1},1,\underbrace{0,\ldots,0}_{J-l}\} \\
&\Omega_2(s) \triangleq \sum_{l=1}^{J} \bar{\rho}_l(1-\bar{\rho}_l)\tilde{\mathfrak{G}}^T_{t,l}(s)\bar{Q}_t(s+1)\tilde{\mathfrak{B}}_{t,l}(s) \\
&\tilde{\mathfrak{B}}_{t,l}(s) \triangleq \begin{bmatrix} WI_l\mathscr{L} \otimes B(s)K_t(s)\Psi_tE(s) \\ WI_l\mathscr{G}\mathscr{L} \otimes B(s)K_t(s)\Psi_tE(s) \end{bmatrix} \\
&\Omega_3(s) \triangleq \sum_{l=1}^{J} \bar{\rho}_l(1-\bar{\rho}_l)\tilde{\mathfrak{G}}^T_{t,l}(s)\bar{Q}_t(s+1)\tilde{\mathfrak{E}}_{t,l}(s) \\
&\tilde{\mathfrak{E}}_{t,l}(s) \triangleq \begin{bmatrix} WI_l\mathscr{L} \otimes B(s)K_t(s) \\ WI_l\mathscr{G}\mathscr{L} \otimes B(s)K_t(s) \end{bmatrix} \\
&\Omega_4(s) \triangleq \sum_{l=1}^{J} \bar{\rho}_l(1-\bar{\rho}_l)\tilde{\mathfrak{B}}^T_{t,l}(s)\bar{Q}_t(s+1)\tilde{\mathfrak{B}}_{t,l}(s) \\
&\Omega_5(s) \triangleq \sum_{l=1}^{J} \bar{\rho}_l(1-\bar{\rho}_l)\tilde{\mathfrak{B}}^T_{t,l}(s)\bar{Q}_t(s+1)\tilde{\mathfrak{E}}_{t,l}(s) \\
&\Omega_6(s) \triangleq \sum_{l=1}^{J} \bar{\rho}_l(1-\bar{\rho}_l)\tilde{\mathfrak{E}}^T_{t,l}(s)\bar{Q}_t(s+1)\tilde{\mathfrak{E}}_{t,l}(s).
\end{aligned}
$$

Proof: By selecting the Lyapunov-like function $V(s) = \chi^T(s)Q_t(s)\chi(s)$, we derive the difference $V(s+1) - V(s)$ along the system trajectory described by (13), as well as its expected value, as follows:

$$
\begin{aligned}
&\mathbb{E}\{V(s+1)-V(s)\} \\
=&\mathbb{E}\Big\{\Big(\big(\mathfrak{A}(s)+\bar{\mathfrak{G}}_t(s)\big)\chi(s)+\bar{\mathfrak{B}}_t(s)v(s)+\mathfrak{C}(s)\omega(s) \\
&+\bar{\mathfrak{E}}_t(s)\nu(s)+\mathfrak{D}_t(s)n(s)\Big)^T\bar{Q}_t(s+1)\Big(\big(\mathfrak{A}(s)+\bar{\mathfrak{G}}_t(s)\big) \\
&\times\chi(s)+\bar{\mathfrak{B}}_t(s)v(s)+\mathfrak{C}(s)\omega(s)+\bar{\mathfrak{E}}_t(s)\nu(s)+\mathfrak{D}_t(s) \\
&\times n(s)\Big)+\Big(\tilde{\mathfrak{G}}_t(s)\chi(s)+\tilde{\mathfrak{B}}_t(s)v(s)+\tilde{\mathfrak{E}}_t(s)\nu(s)\Big)^T \\
&\times\bar{Q}_t(s+1)\Big(\tilde{\mathfrak{G}}_t(s)\chi(s)+\tilde{\mathfrak{B}}_t(s)v(s)+\tilde{\mathfrak{E}}_t(s)\nu(s)\Big) \\
&-\chi^T(s)Q_t(s)\chi(s)\Big\}. \qquad (16)
\end{aligned}
$$

Based on the definitions of $\tilde{\mathfrak{G}}_t(s)$, $\tilde{\mathfrak{B}}_t(s)$, and $\tilde{\mathfrak{E}}_t(s)$, it can be easily obtained that:

$$
\begin{aligned}
&\mathbb{E}\Big\{\Big(\tilde{\mathfrak{G}}_t(s)\chi(s)+\tilde{\mathfrak{B}}_t(s)v(s)+\tilde{\mathfrak{E}}_t(s)\nu(s)\Big)^T\bar{Q}_t(s+1) \\
&\quad\times\Big(\tilde{\mathfrak{G}}_t(s)\chi(s)+\tilde{\mathfrak{B}}_t(s)v(s)+\tilde{\mathfrak{E}}_t(s)\nu(s)\Big)\Big\} \\
=&\mathbb{E}\Big\{\chi^T(s)\tilde{\mathfrak{G}}^T_t(s)\bar{Q}_t(s+1)\tilde{\mathfrak{G}}_t(s)\chi(s)+v^T(s)\tilde{\mathfrak{B}}^T_t(s) \\
&\times\bar{Q}_t(s+1)\tilde{\mathfrak{B}}_t(s)v(s)+\nu^T(s)\tilde{\mathfrak{E}}^T_t(s)\bar{Q}_t(s+1)\tilde{\mathfrak{E}}_t(s) \\
&\times\nu(s)+\mathrm{sym}\Big\{\chi^T(s)\tilde{\mathfrak{G}}^T_t(s)\bar{Q}_t(s+1)\tilde{\mathfrak{B}}_t(s)v(s) \\
&+\chi^T(s)\tilde{\mathfrak{G}}^T_t(s)\bar{Q}_t(s+1)\tilde{\mathfrak{E}}_t(s)\nu(s)+v^T(s)\tilde{\mathfrak{B}}^T_t(s) \\
&\times\bar{Q}_t(s+1)\tilde{\mathfrak{E}}_t(s)\nu(s)\Big\}\Big\}
\end{aligned}
$$

$$
\begin{aligned}
=&\mathbb{E}\Big\{\sum_{l=1}^{J}\bar{\rho}_l(1-\bar{\rho}_l)\Big(\chi^T(s)\tilde{\mathfrak{G}}^T_{t,l}(s)\bar{Q}_t(s+1)\tilde{\mathfrak{G}}_{t,l}(s)\chi(s) \\
&+\nu^T(s)\tilde{\mathfrak{E}}^T_{t,l}(s)\bar{Q}_t(s+1)\tilde{\mathfrak{E}}_{t,l}(s)\nu(s)+v^T(s)\tilde{\mathfrak{B}}^T_{t,l}(s) \\
&\times\bar{Q}_t(s+1)\tilde{\mathfrak{B}}_{t,l}(s)v(s)\Big)+\sum_{l=1}^{J}\bar{\rho}_l(1-\bar{\rho}_l) \\
&\times\Big(\mathrm{sym}\Big\{\chi^T(s)\tilde{\mathfrak{G}}^T_{t,l}(s)\bar{Q}_t(s+1)\tilde{\mathfrak{B}}_{t,l}(s)v(s) \\
&+\chi^T(s)\tilde{\mathfrak{G}}^T_{t,l}(s)\bar{Q}_t(s+1)\tilde{\mathfrak{E}}_{t,l}(s)\nu(s)+v^T(s) \\
&\times\tilde{\mathfrak{B}}^T_{t,l}(s)\bar{Q}_t(s+1)\tilde{\mathfrak{E}}_{t,l}(s)\nu(s)\Big\}\Big)\Big\}. \qquad (17)
\end{aligned}
$$

Furthermore, it follows from (16) that

$$
\begin{aligned}
&\mathbb{E}\Big\{V(s+1)-V(s)\Big\} \\
=&\mathbb{E}\Big\{\chi^T(s)\big(\mathfrak{A}_1(s)+\bar{\mathfrak{G}}_t(s)\big)^T(s)\bar{Q}_t(s+1)\big(\mathfrak{A}_1(s)+\bar{\mathfrak{G}}_t(s)\big) \\
&\times\chi(s)+\chi^T(s)\mathfrak{A}^T_2(s)\bar{Q}_t(s+1)\mathfrak{A}_2(s)\chi(s)+\omega^T(s) \\
&\times\mathfrak{C}^T(s)\bar{Q}_t(s+1)\mathfrak{C}(s)\omega(s)+v^T(s)\bar{\mathfrak{B}}^T_t(s)\bar{Q}_t(s+1) \\
&\times\bar{\mathfrak{B}}_t(s)v(s)+\nu^T(s)\bar{\mathfrak{E}}^T_t(s)\bar{Q}_t(s+1)\bar{\mathfrak{E}}_t(s)\nu(s) \\
&+n^T(s)\mathfrak{D}^T_t(s)\bar{Q}_t(s+1)\mathfrak{D}_t(s)n(s)+\mathrm{sym}\Big\{\chi^{\mathrm{T}}(s) \\
&\times\big(\mathfrak{A}_1(s)+\bar{\mathfrak{G}}_t(s)\big)^T(s)\bar{Q}_t(s+1)\bar{\mathfrak{B}}_t(s)v(s)+\chi^T(s) \\
&\times\big(\mathfrak{A}_1(s)+\bar{\mathfrak{G}}_t(s)\big)^T(s)\bar{Q}_t(s+1)\bar{\mathfrak{E}}_t(s)\nu(s) \\
&+\chi^T(s)\big(\mathfrak{A}_1(s)+\bar{\mathfrak{G}}_t(s)\big)^T(s)\bar{Q}_t(s+1)\mathfrak{C}(s)\omega(s) \\
&+\chi^T(s)\big(\mathfrak{A}_1(s)+\bar{\mathfrak{G}}_t(s)\big)^T(s)\bar{Q}_t(s+1)\mathfrak{D}_t(s)n(s) \\
&+\omega^T(s)\mathfrak{C}^T(s)\bar{Q}_t(s+1)\bar{\mathfrak{B}}_t(s)v(s)+\omega^T(s)\mathfrak{C}^T(s) \\
&\times\bar{Q}_t(s+1)\bar{\mathfrak{E}}_t(s)\nu(s)+\omega^T(s)\mathfrak{C}^T(s)\bar{Q}_t(s+1)\mathfrak{D}_t(s) \\
&\times n(s)+v^T(s)\bar{\mathfrak{B}}^T_t(s)\bar{Q}_t(s+1)\bar{\mathfrak{E}}_t(s)\nu(s) \\
&+v^T(s)\bar{\mathfrak{B}}^T_t(s)\bar{Q}_t(s+1)\mathfrak{D}_t(s)n(s)+\nu^T(s)\bar{\mathfrak{E}}^T_t(s) \\
&\times\bar{Q}_t(s+1)\mathfrak{D}_t(s)n(s)+\sum_{\sigma=1}^{6}\Omega_\sigma(s)\Big\}\Big\} \\
=&\zeta^T(s)\bar{\Xi}_t(s)\zeta(s) \qquad (18)
\end{aligned}
$$

where

$$
\begin{aligned}
&\zeta(s) \triangleq \mathrm{col}\{\chi(s),\omega(s),v(s),\nu(s)\} \\
&\bar{\Xi}_t(s) \triangleq \begin{bmatrix} \bar{\Xi}^t_{11}(s) & \Xi^t_{12}(s) & \Xi^t_{13}(s) & \Xi^t_{14}(s) & \Xi^t_{15}(s) \\ * & \bar{\Xi}^t_{22}(s) & \Xi^t_{23}(s) & \Xi^t_{24}(s) & \Xi^t_{25}(s) \\ * & * & \bar{\Xi}^t_{33}(s) & \Xi^t_{34}(s) & \Xi^t_{35}(s) \\ * & * & * & \bar{\Xi}^t_{44}(s) & \Xi^t_{45}(s) \\ * & * & * & * & \bar{\Xi}^t_{55}(s) \end{bmatrix} \\
&\bar{\Xi}^t_{11}(s) \triangleq \Xi^t_{11}(s)-\mathfrak{F}^T(s)\mathfrak{F}(s) \\
&\bar{\Xi}^t_{22}(s) \triangleq \Xi^t_{22}(s)+\lambda^2 I, \quad \bar{\Xi}^t_{33}(s) \triangleq \Xi^t_{33}(s)+\lambda^2 I \\
&\bar{\Xi}^t_{44}(s) \triangleq \Xi^t_{44}(s)+\lambda^2 I, \quad \bar{\Xi}^t_{55}(s) \triangleq \Xi^t_{55}(s)+\lambda^2 I.
\end{aligned}
$$

Recalling the definition of $\nu(s)$ and the property $\|\nu_{lj}(s)\| \leq \frac{c_{lj}}{b}$, we obtain

$$
\nu^T(s)\nu(s) = \sum_{l=1}^{J}\sum_{j=1}^{n_y}\|\nu_{lj}(s)\|^2 \leq \tilde{c}, \qquad (19)
$$

In consideration of (15), (19) and the finite-horizon H_∞ consensus constraints (14), we can infer that

$$\begin{aligned}&\mathbb{E}\Big\{V(s+1)-V(s)\Big\}\\ \leq&\mathbb{E}\Big\{\zeta^T(s)\bar{\Xi}_t(s)\zeta(s)-\lambda^2\Big(\nu^T(s)\nu(s)-\tilde{c}\Big)+\Big(\|\bar{z}(s)\|^2\\ &-\lambda^2\big(\|v(s)\|^2+\|\omega(s)\|^2+\|n(s)\|^2\big)\Big)-\Big(\|\bar{z}(s)\|^2\\ &-\lambda^2\big(\|v(s)\|^2+\|\omega(s)\|^2+\|n(s)\|^2\big)\Big)\Big\}\\ =&\mathbb{E}\Big\{\zeta^T(s)\Xi_t(s)\zeta(s)-\Big(\|\bar{z}(s)\|^2-\lambda^2\big(\|v(s)\|^2+\|\omega(s)\|^2\\ &+\|n(s)\|^2+\tilde{c}\big)\Big)\Big\}\\ \leq&-\mathbb{E}\Big\{\|\bar{z}(s)\|^2-\lambda^2\Big(\|v(s)\|^2+\|\omega(s)\|^2+\|n(s)\|^2+\tilde{c}\Big)\Big\}\end{aligned} \tag{20}$$

and, subsequently, by summing both sides of (20) with respect to s from 0 to $\mathcal{S}-1$, we arrive at

$$\begin{aligned}&\mathbb{E}\Big\{\sum_{s=0}^{\mathcal{S}-1}\Big(V(s+1)-V(s)\Big)\Big\}\\ \leq&-\mathbb{E}\Big\{\sum_{s=0}^{\mathcal{S}-1}\Big(\|\bar{z}(s)\|^2-\lambda^2\big(\|v(s)\|^2+\|\omega(s)\|^2+\|n(s)\|^2\\ &+\tilde{c}\big)\Big)\Big\}.\end{aligned} \tag{21}$$

Then, from $\bar{Q}_t(0)\leq\lambda^2\Pi$ and $V(s+1)>0$, it is straightforward to obtain:

$$\begin{aligned}\mathbb{E}\Big\{\|\bar{z}(s)\|^2\Big\}\leq&\mathbb{E}\Big\{\sum_{s=0}^{\mathcal{S}-1}\lambda^2\big(\|v(s)\|^2+\|\omega(s)\|^2+\|n(s)\|^2\\ &+\tilde{c}\big)+\lambda^2\chi^T(0)(I_J\otimes\Pi)\chi(0)\Big\}.\end{aligned} \tag{22}$$

Thus, the augmented system (13) satisfies the finite-horizon H_∞ consensus constraint defined in (14) over the finite horizon. ■

B. Design of the Controller

In this section, the gain matrix $K_t(s)$ in controller (8) is designed to ensure that the stochastic MAS (1) satisfies the finite-horizon H_∞ performance. To facilitate the subsequent derivation, the following lemma is presented based on the description in [21].

Lemma 1: [21] For a full-column-rank matrix $B(s)\in\mathbb{R}^{n_x\times n_u}$, there exist orthogonal matrices $\Lambda(s)\in\mathbb{R}^{n_x\times n_x}$ and $\Theta(s)\in\mathbb{R}^{n_u\times n_u}$ such that the following singular value decomposition holds:

$$B(s)=\Lambda(s)\begin{bmatrix}\Sigma(s)\\0\end{bmatrix}\Theta^T(s)=\begin{bmatrix}\Lambda_1^T(s)\\\Lambda_2^T(s)\end{bmatrix}^T\begin{bmatrix}\Sigma(s)\\0\end{bmatrix}\Theta^T(s),$$

where $\Lambda_1(s)\in\mathbb{R}^{n_x\times n_u}$ and $\Lambda_2(s)\in\mathbb{R}^{n_x\times(n_x-n_u)}$ are submatrices of $\Lambda(s)$, and $\Sigma(s)=\operatorname{diag}\{\varepsilon_1(s),\ldots,\varepsilon_{n_u}(s)\}$ contains the nonzero singular values of $B(s)$. If matrix $\bar{Q}_t(k+1)$ adopts the block-diagonal structure:

$$\bar{Q}_t(s+1)=\begin{bmatrix}\Lambda_1^T(s)\\\Lambda_2^T(s)\end{bmatrix}^T\begin{bmatrix}P_t^1(s+1)&0\\0&P_t^2(s+1)\end{bmatrix}\begin{bmatrix}\Lambda_1^T(s)\\\Lambda_2^T(s)\end{bmatrix}$$

or equivalently,

$$\bar{Q}_t(s+1)=\Lambda_1(s)P_t^1(s+1)\Lambda_1^T(s)+\Lambda_2(s)P_t^2(s+1)\Lambda_2^T(s),$$

with $P_t^1(s+1)>0$ and $P_t^2(s+1)>0$, then there exists a nonsingular matrix $\tilde{Q}_t(s+1)\in\mathbb{R}^{n_u\times n_u}$ satisfying

$$B(s)\tilde{Q}_t(s+1)=\bar{Q}_t(s+1)B(s),$$

which is explicitly given by:

$$\tilde{Q}_t(s+1)=\Theta^T(s)\Sigma^{-1}(s)P_t^1(s+1)\Sigma(s)\Theta(s).$$

Theorem 2: For any agent $t\in\Upsilon$, consider a directed communication graph $\mathcal{G}$, disturbance attenuation level $\lambda>0$, and positive definite symmetric matrices Π_1, Π_2. The stochastic multi-agent system (13) achieves H_∞ consensus under constraints (14) if there exist a matrix sequence $\{\tilde{Q}_t(s)\}_{s\in[0,\mathcal{S}-1]}$; positive definite matrix sequences $P_t^1(s),P_t^2(s),Q_t(s)_{s\in[0,\mathcal{S}-1]}$ satisfying initial conditions: $P_t^1(0)\leq\lambda^2\Pi_1$, $P_t^2(0)\leq\lambda^2\Pi_2$; a weighted coupling term $\bar{Q}_t(s)=\sum_{m=1}^{n_y}p_{tm}Q_m(s)$, $(t,m\in\Upsilon)$ with structural decomposition $\bar{Q}_t(s+1)=\Lambda_1(s)P_t^1(s+1)\Lambda_1^{\mathsf{T}}(s)+\Lambda_2(s)P_t^2(s+1)\Lambda_2^{\mathsf{T}}(s)$ such that the following RLMI is feasible:

$$\tilde{\Xi}_t=\begin{bmatrix}\tilde{\Xi}_t^1&*\\\tilde{\Xi}_t^2&\tilde{\Xi}_t^3\end{bmatrix}<0 \tag{23}$$

where

$$\begin{aligned}\tilde{\Xi}_t^1\triangleq&\operatorname{diag}\Big\{-Q_t(s)+\mathfrak{F}^T(s)\mathfrak{F}(s),-\lambda^2I,-\lambda^2I,-\lambda^2I,\\&-\lambda^2I\Big\}\\ \tilde{\Xi}_t^2\triangleq&\begin{bmatrix}\tilde{\Xi}_t^{21}&\tilde{\Xi}_t^{22}&\tilde{\Xi}_t^{23}&\tilde{\Xi}_t^{24}&\tilde{\Xi}_t^{25}\\\tilde{\Xi}_t^{26}&0&0&0&0\\\tilde{\Xi}_t^{27}&0&\tilde{\Xi}_t^{28}&\tilde{\Xi}_t^{29}&0\\\tilde{\Xi}_t^{210}&0&\tilde{\Xi}_t^{211}&\tilde{\Xi}_t^{212}&0\end{bmatrix}\\ \tilde{\Xi}_t^{21}\triangleq&\operatorname{diag}\Big\{I_J\otimes\bar{Q}_t(s+1)A(s)+W\bar{\rho}\mathcal{L}\otimes B(s)\tilde{Q}_t(s+1)\\&\times\Psi_tD(s),I_J\otimes\bar{Q}_t(s+1)A(s)+W\bar{\rho}\mathcal{G}\mathcal{L}\otimes\\&\times B(s)\tilde{Q}_t(s+1)\Psi_tD(s)\Big\}\\ \tilde{\Xi}_t^{22}\triangleq&\begin{bmatrix}I_J\otimes\bar{Q}_t(s+1)C(s)\\\mathcal{G}\otimes\bar{Q}_t(s+1)C(s)\end{bmatrix}\\ \tilde{\Xi}_t^{23}\triangleq&\begin{bmatrix}W\bar{\rho}\mathcal{L}\otimes B(s)\tilde{Q}_t(s+1)\Psi_tE(s)\\W\bar{\rho}\mathcal{G}\mathcal{L}\otimes B(s)\tilde{Q}_t(s+1)\Psi_tE(s)\end{bmatrix}\\ \tilde{\Xi}_t^{24}\triangleq&\begin{bmatrix}W\bar{\rho}\mathcal{L}\otimes B(s)\tilde{Q}_t(s+1)\\W\bar{\rho}\mathcal{G}\mathcal{L}\otimes B(s)\tilde{Q}_t(s+1)\end{bmatrix}\\ \tilde{\Xi}_t^{25}\triangleq&\begin{bmatrix}H(s)\mathcal{L}\otimes B(s)\tilde{Q}_t(s+1)\\H(s)\mathcal{G}\mathcal{L}\otimes B(s)\tilde{Q}_t(s+1)\end{bmatrix}\\ \tilde{\Xi}_t^{26}\triangleq&\operatorname{diag}\Big\{I_J\otimes\bar{Q}_t(s+1)G(s),I_J\otimes\bar{Q}_t(s+1)G(s)\Big\}\\ \tilde{\Xi}_t^{27}\triangleq&\sqrt{\rho_1^*}\operatorname{diag}\Big\{WI_1\mathcal{L}\otimes B(s)\tilde{Q}_t(s+1)\Psi_tD(s),\end{aligned}$$

$$WI_1\mathcal{G}\mathcal{L}\otimes B(s)\tilde{Q}_t(s+1)\Psi_t D(s)\Big\}$$

$$\tilde{\Xi}_t^{28}\triangleq\sqrt{\rho_1^*}\begin{bmatrix}WI_1\mathcal{L}\otimes B(s)\tilde{Q}_t(s+1)\Psi_t E(s)\\WI_1\mathcal{G}\mathcal{L}\otimes B(s)\tilde{Q}_t(s+1)\Psi_t E(s)\end{bmatrix}$$

$$\tilde{\Xi}_t^{29}\triangleq\sqrt{\rho_1^*}\begin{bmatrix}WI_1\mathcal{L}\otimes B(s)\tilde{Q}_t(s+1)\\WI_1\mathcal{G}\mathcal{L}\otimes B(s)\tilde{Q}_t(s+1)\end{bmatrix}$$

$$\tilde{\Xi}_t^{210}\triangleq\sqrt{\rho_2^*}\mathrm{diag}\Big\{WI_2\mathcal{L}\otimes B(s)\tilde{Q}_t(s+1)\Psi_t D(s),\quad WI_2\mathcal{G}\mathcal{L}\otimes B(s)\tilde{Q}_t(s+1)\Psi_t D(s)\Big\}$$

$$\tilde{\Xi}_t^{211}\triangleq\sqrt{\rho_2^*}\begin{bmatrix}WI_2\mathcal{L}\otimes B(s)\tilde{Q}_t(s+1)\Psi_t E(s)\\WI_2\mathcal{G}\mathcal{L}\otimes B(s)\tilde{Q}_t(s+1)\Psi_t E(s)\end{bmatrix}$$

$$\tilde{\Xi}_t^{212}\triangleq\sqrt{\rho_2^*}\begin{bmatrix}WI_2\mathcal{L}\otimes B(s)\tilde{Q}_t(s+1)\\WI_2\mathcal{G}\mathcal{L}\otimes B(s)\tilde{Q}_t(s+1)\end{bmatrix}$$

$$\tilde{\Xi}_t^{3}\triangleq\mathrm{diag}\Big\{I_J\otimes\bar{Q}_t(s+1),I_J\otimes\bar{Q}_t(s+1),I_J\otimes\bar{Q}_t(s+1),\quad I_J\otimes\bar{Q}_t(s+1)\Big\},\quad \rho_l^*\triangleq\bar{\rho}_l\big(1-\bar{\rho}_l\big).$$

Moreover, the control gain matrix $K_t(s)$ can be designed by

$$K_t(s)=\Theta(s)\Sigma(s)\big(P_t^1(s+1)\big)^{-1}\Sigma^{-1}(s)\Theta^T(s)\tilde{Q}_t(s+1)\tag{24}$$

where $\Theta(s)$, $\Sigma(s)$, and $\Lambda(s)$ are as defined in Lemma 1.

Proof: From Lemma 1, it can be directly deduced that $B(s)\tilde{Q}_t(s+1)=\bar{Q}_t(s+1)B(s)$. By setting $\tilde{Q}_t(s)\triangleq\bar{Q}_t(s+1)K_t(s)$, and applying the Schur complement lemma to (15) in Theorem 1, the inequality (23) is derived, thereby completing the proof. ■

Based on Theorem 1 and Theorem 2, we propose the following SCP-DaF-based Finite-Horizon H_∞ consensus controller design (FHCCD) algorithm. This algorithm allows for the computation of the gain $K_t(s)$ at each time instant $s\in[0,\mathcal{S}-1]$.

SCP-DaF-based FHCCD Algorithm	
Step 1	Set $s=0$, given parameters $\lambda>0$ and $\Pi>0$, then determine the initial values $P_t^1(0)$ and $P_t^2(0)$ according to the inequalities: $P_t^1(0)\le\lambda^2\Pi_1$, $P_t^2(0)\le\lambda^2\Pi_2$.
Step 2	Solve RLMI (23) to obtain $P_t^1(s+1)$, $P_t^2(s+1)$, and $\tilde{Q}_t(s+1)$, then compute the gain $K_t(s)$ at step s using (24).
Step 3	If $s\le\mathcal{S}-1$, increment $s=s+1$ and return to Step 2; otherwise, proceed to Step 4.
Step 4	Stop.

Remark 3: In Theorem 1, a sufficient condition is established for system (13) to satisfy the H_∞ performance criterion by utilizing RLMIs and stochastic analysis techniques. Building on this result, an RLMI formulation is presented in Theorem 2 for computing the parameter matrices through the application of the Schur complement lemma. Subsequently, the feasible controller gain $K_t(s)$ is obtained via (24), and the SCP-DaF-based FHCCD Algorithm is proposed to compute the controller gain $K_t(s)$. From an implementation viewpoint, the proposed FHCCD algorithm is mainly intended for offline controller synthesis. For the MAS studied in this paper, which has a fixed system size, the overall computational cost grows approximately linearly with S, because the recursive LMI feasibility problem is solved at each time instant $s\in[0,S-1]$. With an increasing number of agents, the cost of solving each RLMI grows more significantly due to the enlarged matrix dimensions and coupled constraints.

Remark 4: Compared with existing literature, this paper differs in the following aspects: 1) It considers stochastic scheduling, DaF relay communications, encoding-decoding errors, and random packet losses in a unified framework; 2) The scheduled signals are further encoded, decoded, and forwarded through relay nodes, which has not been addressed in previous studies; 3) It focuses on distributed finite-horizon H_∞ consensus control, where the consensus error among agents is used as the main performance index; 4) Packet losses in both the decoding-to-relay and relay-to-controller stages are explicitly considered, which better reflects practical IoT communication environments. Based on this joint SCP-DaF communication model, an augmented stochastic consensus-error system is constructed, recursive LMI-based sufficient conditions are derived, and a scheduling-dependent controller design algorithm is developed to guarantee finite-horizon H_∞ consensus performance.

IV. Illustrative Example

In this section, the effectiveness of the SCP-DaF-based controller (8) is verified through the following numerical example.

Consider a multi-agent system consisting of three agents, where the communication topology is represented by a directed graph $\mathcal{G}$. The set of nodes is $\mathcal{J}=1,2,3$, and the corresponding adjacency matrix $\mathcal{A}$ is given as follows:

$$\mathcal{A}=\begin{bmatrix}0&1&1\\1&0&1\\1&1&0\end{bmatrix}.$$

For the stochastic MAS (1), the parameters are chosen as follows:

$$A(s)=\begin{bmatrix}-\sin(0.4s)&-0.5\\-0.1&-0.4\end{bmatrix}$$
$$B(s)=\begin{bmatrix}0.5&0.3\cos(3s)\\0.2&0.4\end{bmatrix}$$
$$C(s)=\begin{bmatrix}0.2&0\\0&0.1\sin(2s)\end{bmatrix}$$
$$D(s)=\begin{bmatrix}0.3\cos(3s)&0.22\\\cos(s)&0.2\end{bmatrix}$$
$$E(s)=\begin{bmatrix}-0.01&0.03\\-0.01&0.02\end{bmatrix}$$
$$F(s)=\begin{bmatrix}0.3&0\\0&0.1\end{bmatrix},\quad G(s)=\begin{bmatrix}0&0.01\\0.01&0\end{bmatrix}.$$

The updating matrix is set as

$$\mathrm{P}=\begin{bmatrix}0.4&0.6\\0.5&0.5\end{bmatrix},$$

the disturbance attenuation level is chosen as $\lambda=0.8$, the packet loss parameters are set as $\bar{\alpha}_l=0.7$ and $\bar{\beta}_l=0.7$, corresponding to a packet loss rate of 30% in the transmission from the decoder to the relay and from the relay to the controller, respectively, for each agent at each time step. The remaining parameter settings are given as follows:

$$\Pi = 15I, \quad W_l = 2, \quad c_{lj} = 0.1, \quad b = 20, \quad H_l(s) = 0.1.$$

The augmented system (10) is obtained from system (1) under the simultaneous influence of SCP and DaF. The exogenous disturbances $\omega_l(s)$, $v_l(s)$, and $n_l(s)$, as well as the initial conditions, are selected as follows:

$$\begin{aligned}
\omega_1(s) &= \begin{bmatrix} 0.8\cos(1.2s) \\ 0.8\cos(1.2s) \end{bmatrix}, \quad \omega_2(s) = \begin{bmatrix} 0.8\cos(0.5s) \\ 0.8\cos(0.5s) \end{bmatrix} \\
\omega_3(s) &= \begin{bmatrix} 0.8\cos(1.3s) \\ 0.8\cos(1.3s) \end{bmatrix}, \quad v_1(s) = \begin{bmatrix} 0.1\sin(1.2s) \\ 0.1\sin(1.2s) \end{bmatrix} \\
v_2(s) &= \begin{bmatrix} 0.1\sin(0.7s) \\ 0.1\sin(0.7s) \end{bmatrix}, \quad v_3(s) = \begin{bmatrix} 0.1\cos(s) \\ 0.1\cos(s) \end{bmatrix} \\
n_l(s) &= \begin{bmatrix} \frac{0.1}{\sqrt{1+s}} \\ \frac{0.1}{\sqrt{1+s}} \end{bmatrix} \quad (l \in \mathcal{G}), \quad x_1(0) = \begin{bmatrix} 1 \\ -6.5 \end{bmatrix} \\
x_2(0) &= \begin{bmatrix} -1 \\ 3 \end{bmatrix}, \quad x_3(0) = \begin{bmatrix} 2 \\ 4 \end{bmatrix}.
\end{aligned}$$

Additionally, we assume that $x_l(-3) = x_l(-2) = x_l(-1) = x_l(0)$ for $l = 1, 2, 3$. The remaining parameters are set as follows:

$$\epsilon = 0.05, \quad n_{1l}(s) = \frac{0.1\cos(s)}{(s+1)^2}, \quad n_{2l}(s) = \frac{0.15\cos(s)}{(s+1)^2}.$$

Using the YALMIP toolbox, the feasible solutions to LMIs (23) and the corresponding H_∞ gain matrices are obtained for $s = 3$ as follows:

$$\begin{aligned}
P_1^1 &= 1.0343, \quad \tilde{Q}_1 = \begin{bmatrix} 0.0410 & 0.0122 \\ -0.0000 & -0.0000 \end{bmatrix} \\
\tilde{K}_1 &= \begin{bmatrix} 0.0396 & 0.0118 \\ -0.0000 & -0.0000 \end{bmatrix} \\
P_2^1 &= 1.0329, \quad \tilde{Q}_2 = \begin{bmatrix} 0.0000 & -0.0000 \\ -0.0357 & 0.0156 \end{bmatrix} \\
\tilde{K}_2 &= \begin{bmatrix} 0.0000 & -0.0000 \\ -0.0345 & 0.0151 \end{bmatrix}.
\end{aligned}$$

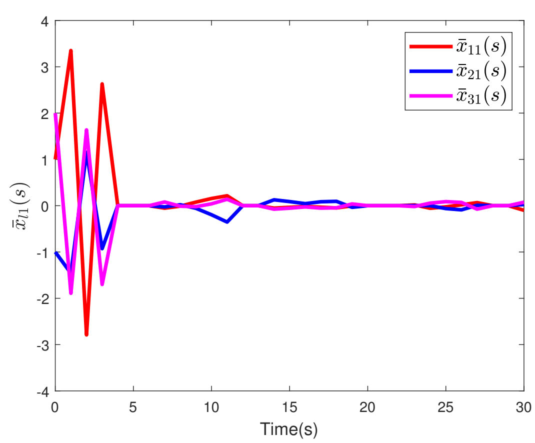

Fig. 1. Trajectories of the agent state deviation $\bar{x}_{l1}(s), l \in \mathcal{G}$.

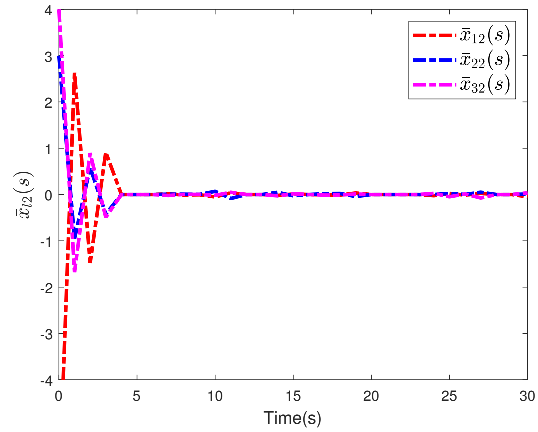

Fig. 2. Trajectories of the agent state deviation $\bar{x}_{l2}(s), l \in \mathcal{G}$.

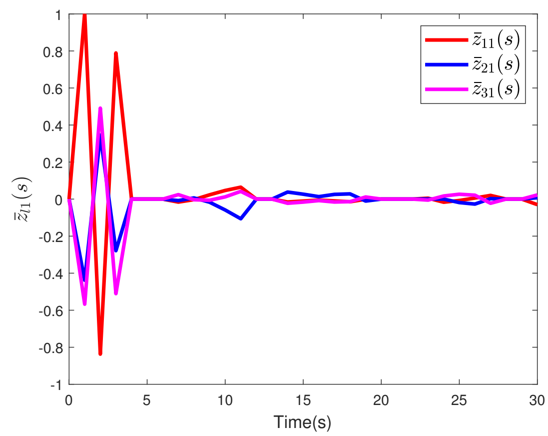

Fig. 3. Trajectories of the controlled output deviation $\bar{z}_{l1}(s), l \in \mathcal{G}$.

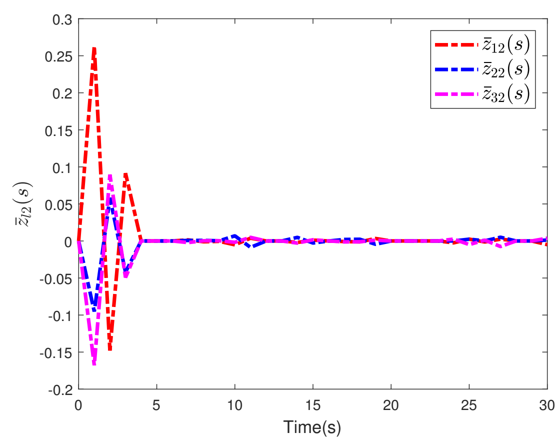

Fig. 4. Trajectories of the controlled output deviation $\bar{z}_{l2}(s), l \in \mathcal{G}$.

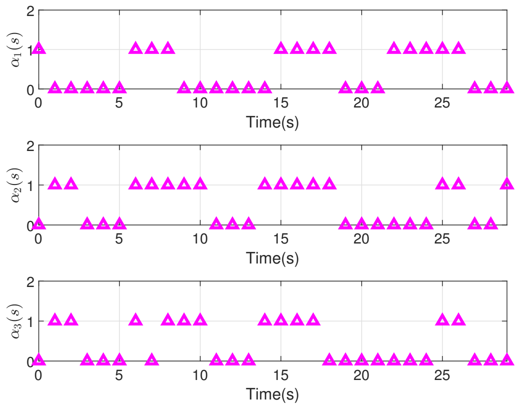

Fig. 5. The values of $\alpha_l(s), l \in \mathcal{G}$.

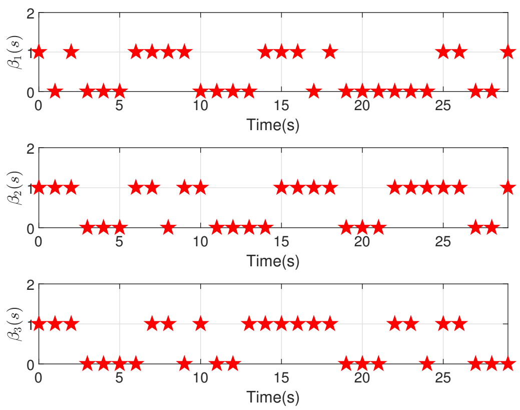

Fig. 6. The values of $\beta_l(s), l \in \mathcal{G}$.

According to the SCP-DaF-based FHCCD algorithm, the control gain matrix $K_t(s)$ is computed at each time step s. The effectiveness of the control strategy, which incorporates the SCP and DaF relay protocols, is verified through simulation results presented in Figs. 1–6. Specifically, Figs. 1 and 2 illustrate the evolution trajectories of the deviation $\bar{x}_l(s)$ between the individual agent states $x_l(s)$ and their average. Figs. 3 and 4 depict the trajectories of the deviation $\bar{z}_l(s)$ between $z_l(s)$ and its average. Collectively, these four figures demonstrate that consensus is achieved, indicating that the states of all agents tend to synchronize over time. Furthermore, Figs. 5 and 6 present the occurrence of stochastic packet dropouts in the communication network. In these two figures, markers indicate successful data transmission when $\alpha_l(s) = 1$ or $\beta_{2l}(s) = 1$; otherwise, when $\alpha_l(s) = 0$ or $\beta_{2l}(s) = 0$, agent l experiences a packet loss. These results confirm the effectiveness of the controller (8) for the stochastic MAS system (1) under the influence of the SCP protocol and the DaF relay mechanism with random packet losses.

V. Conclusion

In this paper, the finite-horizon H_∞ consensus control problem has been investigated for IoT-enabled MASs with random parameters under the joint influence of SCP scheduling, DaF relay-assisted communications, and stochastic packet losses. A unified SCP-DaF communication framework has been developed, where the transmitted signals are first scheduled by the SCP and then encoded, decoded, and forwarded through relay nodes. Based on this framework, an augmented stochastic consensus-error system has been constructed, and sufficient conditions have been derived in terms of RLMIs to guarantee the prescribed finite-horizon H_∞ consensus performance. A corresponding FHCCD algorithm has also been proposed to compute the scheduling-dependent controller gains. Simulation results have demonstrated that the proposed controller can effectively drive the agent-state and controlled-output deviations to consensus despite external disturbances and random packet losses. Nevertheless, the approach assumes known packet-loss probabilities, a fixed communication topology, and centralized RLMI-based controller computation, which may limit its scalability and adaptability in large or dynamic IoT systems. Future research will consider finite-horizon consensus control with unknown or time-varying packet-loss probabilities, distributed and structure-exploiting RLMI algorithms, and experimental validation on practical IoT-enabled multi-agent platforms.

References

[1] H. Shen, Y. Wang, J. Wu, J. H. Park and J. Wang, Secure Control for Markov Jump Cyber-Physical Systems Subject to Malicious Attacks: A Resilient Hybrid Learning Scheme, *IEEE Transactions on Cybernetics*, vol. 54, no. 11, pp. 7068-7079, 2024.

[2] J. Wang, D. Wang, H. Yan and H. Shen, Composite Antidisturbance $\mathscr{H}_\infty$ Control for Hidden Markov Jump Systems With Multi-Sensor Against Replay Attacks, *IEEE Transactions on Automatic Control*, vol. 69, no. 3, pp. 1760-1766, 2024.

[3] W. Chen, J. Hu, Z. Wu and S. Ma, A survey on fault detection for networked systems under communication constraints, *Systems Science & Control Engineering, vol. 13, no. 1, art. no. 2460434, 2025.*

[4] M. Thummalapeta and Y. Liu, Survey of containment control in multi-agent systems: concepts, communication, dynamics, and controller design, *International Journal of Systems Science*, vol. 54, no. 14, pp. 2809-2835, 2023.

[5] J. T. Mawanza, M. Manganda and O. E. Ijiga, A novel fixed-time control scheme for multi-UAV wildfire tracking with dynamic reconfiguration and fault tolerance, *Systems Science & Control Engineering*, vol. 13, no. 1, art. no. 2587840, 2025.

[6] L. Zheng, H. Ren, D. Yao and H. Li, Event-based finite-time sliding mode consensus tracking control for multiagent systems with actuator failures, *International Journal of Systems Science*, vol. 56, no. 2, pp. 303–317, 2025.

[7] L. Yu, J. Ding, H. Peng, Y. Liu and Y. Liu, Sampled-data based containment control for a class of nonlinear multiagent systems with dynamic leaders and control saturation, *International Journal of Network Dynamics and Intelligence*, vol. 4, no. 2, art. no. 100011, Jun. 2025.

[8] A. A. Amin, A. Mubarak and H. U. Manzoor, Design of intelligent vehicular and sensor communication network: a comprehensive survey, *Systems Science & Control Engineering*, vol. 13, no. 1, art. no. 2529187, 2025.

[9] M. Shah, A. Wahid, E. Barrett and K. Mason, Multi-agent systems in Peer-to-Peer energy trading: A comprehensive survey, *Engineering Applications of Artificial Intelligence*, vol. 132, pp. 107847, 2024.

[10] L. Zou, B. Song, J. Suo, N. Li and C. Wang, A survey on outlier-resistant state estimation and its applications, *Systems Science & Control Engineering*, vol. 13, no. 1, art. no. 2474471, 2025.

[11] M. Zhao, J. Xi, L. Wang, K. Xia and Y. Zheng, Edge-based adaptive secure consensus for nonlinear multiagent systems with communication link attacks, *Neurocomputing*, vol. 551, pp. 126505, 2023.

[12] Y. Li, K. Li and S. Tong, An observer-based fuzzy adaptive consensus control method for nonlinear multiagent systems, *IEEE Transactions on Fuzzy Systems*, vol. 30, no. 11, pp. 4667-4678, 2022.

[13] L. Ma, F. Zhu and X. Zhao, Human-in-the-loop consensus control for multiagent systems with external disturbances, *IEEE Transactions on Neural Networks and Learning Systems*, vol. 35, no. 8, pp. 11024-11034, 2023.

[14] X.-J. Peng, Y. He, H. Li and S. Tian, Consensus Control and Optimization of Time-Delayed Multiagent Systems: Analysis on Different Order-Reduction Methods, *IEEE Transactions on Systems, Man, and Cybernetics: Systems*, vol. 55, no. 1, pp. 780-791, 2025.

[15] G. Wang, Z. Zuo and C. Wang, Robust consensus control of second-order uncertain multiagent systems with velocity and input constraints, *Automatica*, vol. 157, pp. 111226, 2023.

[16] X. Wu, B. Mao, X. Wu and J. Lu, Dynamic event-triggered leader-follower consensus control for multiagent systems, *SIAM Journal on Control and Optimization*, vol. 60, no. 1, pp. 189-209, 2022.

[17] H. Zhao, H. Wang, N. Xu, X. Zhao and S. Sharaf, Fuzzy approximation-based optimal consensus control for nonlinear multiagent systems via adaptive dynamic programming, *Neurocomputing*, vol. 553, pp. 126529, 2023.

[18] L. Yu, J. Ding, H. Peng, Y. Liu and Y. Liu, Sampled-data based containment control for a class of nonlinear multiagent systems with dynamic leaders and control saturation, *International Journal of Network Dynamics and Intelligence*, vol. 4, no. 2, art. no. 100011, Jun. 2025.

[19] S. Yuan, L. Ma and C. Gao, Probability-guaranteed consensus control for nonlinear multi-agent systems under bit flips, *International Journal of Network Dynamics and Intelligence*, vol. 4, no. 3, art. no. 100020, Sept. 2025.

[20] L. Zheng, H. Ren, D. Yao and H. Li, Event-based finite-time sliding mode consensus tracking control for multiagent systems with actuator failures, *International Journal of Systems Science*, vol. 56, no. 2, pp. 303–317, 2025.

[21] F. Han, G. Wei, D. Ding and Y. Song, Finite-horizon H_∞-consensus control for multi-agent systems with random parameters: The local condition case, *Journal of the Franklin Institute*, vol. 354, no. 14, pp. 6078-6097, 2017.

[22] B. Zhou, J. H. Park, Y. Yang, R. Hao and Y. Jiao, Prescribed-time consensus of time-varying open multi-agent systems with delays on time scales, *Information Sciences*, vol. 680, pp. 120957, 2024.

[23] Z. Sun and C. Han, Linear state estimation for multi-rate NCSs with multi-channel observation delays and unknown Markov packet losses, *International Journal of Network Dynamics and Intelligence*, vol. 4, no. 1, art. no. 100005, Mar. 2025.

[24] X. Liu, Z. Ling and Y. Zhang, Torus-event-based sliding mode control for networked interval type-2 fuzzy systems under deception attacks, *International Journal of Network Dynamics and Intelligence*, vol. 4, no. 1, art. no. 100003, Mar. 2025.

[25] J. Song, F. Han, H. Fu and H. Liu, Finite-horizon distributed H_∞-consensus control of time-varying multi-agent systems with Round-Robin protocol, *Neurocomputing*, vol. 364, pp. 219-226, 2019.

[26] X. Meng, H. Wang, Y. Li and Y. Shen, Unscented Kalman filtering for nonlinear systems with stochastic nonlinearities under FlexRay protocol, *International Journal of Network Dynamics and Intelligence*, vol. 4, no. 2, art. no. 100010, Jun. 2025.

[27] Y. Song, J. Zhang, F. Han, Y. Shen, H. Dong and Z. Hu, Scalable distributed estimation for time-varying system with generalized weighted try-once-discard and round-robin protocols, *IEEE Sensors Journal*, vol. 25, no. 16, pp. 31653-31663, Aug. 2025.

[28] Y. Wang, Z. Wang, L. Zou and H. Dong, Observer-based fuzzy PID tracking control under try-once-discard communication protocol: An affine fuzzy model approach, *IEEE Transactions on Fuzzy Systems*, vol. 32, no. 4, pp. 2352-2365, 2024.

[29] C. Li, Y. Liu, M. Gao and L. Sheng, Fault-tolerant formation consensus control for time-varying multi-agent systems with stochastic communication protocol, *International Journal of Network Dynamics and Intelligence*, vol. 3, no. 1, pp. 100004, 2024.

[30] S. Liu, L. Wang, Y. Zhang, Y.-A. Wang and H. Dong, Recursive filtering of networked systems with communication protocol scheduling: a survey, *International Journal of Systems Science*, vol. 56, no. 11, pp. 2499–2516, 2025.

[31] J. Li, Z. Wang and J. Hu, Cubature Kalman fusion filtering under stochastic communication protocol: Tackling dynamical bias, scheduling probability and channel noise, *Information Fusion*, vol. 113, pp. 102610, 2025.

[32] S. Liu, J. Cheng, H. Yan and D. Zhang, Adaptive Neural Sliding-Mode Control for Fuzzy Singularly Perturbed Systems: Sojourn-Probability-Based Stochastic Communication Protocol, *IEEE Transactions on Cybernetics*, vol. 54, no. 10, pp. 6095-6104, 2024.

[33] W. Zhang, Y. Zhao, H. Wang and Z. Yang, Robust model predictive control for polyhedral uncertain systems under relay and redundancy protocol, *International Journal of Systems Science*, vol. 56, no. 8, pp. 1617–1632, 2025.

[34] S. Cai and J. Liang, Recursive filtering for nonlinear systems with relay communication, energy harvesting and correlated noises, *International Journal of Network Dynamics and Intelligence*, vol. 4, no. 3, art. no. 100021, Sept. 2025.

[35] W. Le, B. Shen, L. Zou, J. Sun, Stubborn state estimation for time-delay systems with relay communication network: the half-duplex case, *Journal of the Franklin Institute*, vol. 362, no. 2, art. no. 107465, Jan. 2025.

[36] T. Liu, Z. Wang, Y. Liu and R. Wang, Recursive remote state estimation for stochastic complex networks with degraded measurements and amplify-and-forward relays, *IEEE Transactions on Network Science and Engineering*, vol. 12, no. 2, pp. 1343-1356, 2025.

[37] C. Liang, D. He and C. Xu, Distributed H_∞ moving horizon estimation over energy harvesting sensor networks, *International Journal of Systems Science*, vol. 56, no. 15, pp. 3743–3757, 2025.

[38] D. Dai, J. Li, J. Zhang, B. Jiang and H. Dong, Energy-harvesting recursive filtering for delayed systems with amplify-and-forward relays: cooperative communication manner, *Journal of the Franklin Institute*, vol. 361, no. 18, art. no. 107265, Dec. 2024.

[39] J. Hu, J. Li, H. Yan and H. Liu, Optimized distributed filtering for saturated systems with amplify-and-forward relays over sensor networks: a dynamic event-triggered approach, *IEEE Transactions on Neural Networks and Learning Systems*, vol. 35, no. 12, pp. 17742–17753, Dec. 2024.

[40] M. Shi, L. Ma and X. Yi, Recursive state estimation for complex networks with energy harvesting constraints and decode-and-forward relays, *IEEE Transactions on Systems, Man, and Cybernetics: Systems*, vol. 55, no. 8, pp. 5491–5502, Aug. 2025.

[41] H. Tan, B. Shen, Q. Li and H. Liu, Recursive filtering for stochastic systems with filter-and-forward successive relays, *IEEE/CAA Journal of Automatica Sinica*, vol. 11, no. 5, pp. 1202–1212, May. 2024.

[42] Y. Gao, J. Hu, K. Chi, C. Jia and J. Qi, A variance-constrained method to encoding-decoding H_∞ state estimation for memristive neural networks with energy harvesting sensor, *Neurocomputing*, vol. 579, art. no. 127448, Apr. 2024.

[43] G. Li, Z. Wang, X. Bai, Z. Zhao and Y. Wang, Recursive state estimation for permanent magnet synchronous motors with sensor degradations under encoding-decoding cchemes, *IEEE Transactions on Industrial Informatics*, vol. 20, no. 12, pp. 13687-13695, 2024.

[44] L. Wang, Z. Wang, S. Liu and D. Peng, Unscented Kalman filtering over full-duplex relay networks under binary encoding schemes, *IEEE Transactions on Automatic Control*, vol. 70, no. 5, pp. 3441-3448, 2025.

[45] X. Meng, Z. Wang, F. Wang, and Y. Chen, State Estimation for Nonlinear Complex Dynamical Networks With Random Coupling Strengths: A Decode-and-Forward Relay-Based Strategy, *IEEE Transactions on Systems, Man, and Cybernetics: Systems*, vol. 54, no. 8, pp. 4749-4760, 2024.

[46] L. Zou, Z. Wang, B. Shen and H. Dong, Recursive state estimation in relay channels with enhanced security against eavesdropping: An innovative encryption–decryption framework, *Automatica*, vol. 174, pp. 112159, 2025.

[47] M. Shen, Y. Gu, S. Zhu, G. Zong and X. Zhao, Mismatched Quantized H_∞ Output-Feedback Control of Fuzzy Markov Jump Systems With a Dynamic Guaranteed Cost Triggering Scheme, *IEEE Transactions on Fuzzy Systems*, vol. 32, no. 4, pp. 1681-1692, 2025.

[48] M. Shen, S. K. Nguang, C. K. Ahn and Q.-G. Wang, Robust H_2 Control of Linear Systems With Mismatched Quantization, *IEEE Transactions on Automatic Control*, vol. 64, no. 4, pp. 1702-1709, 2019.

[49] L. Zou, Z. Wang, H. Gao and F. E. Alsaadi, Finite-horizon $\mathscr{H}_\infty$ consensus control of time-varying multiagent systems with stochastic communication protocol, *IEEE Transactions on cybernetics*, vol. 47, no. 8, pp. 1830-1840, 2017.

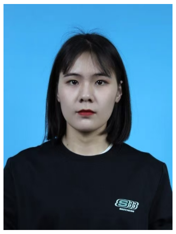

Jie Ban received the B.Sc. degree in Mathematics and Applied Mathematics from Shangqiu Normal University, Shangqiu, China, in 2020, and the M.S. degree in Mathematics from the University of Science and Technology Liaoning, Anshan, China, in 2023.

She is currently a Ph.D. student in Control Science and Engineering at the School of Electronic and Information Engineering, University of Science and Technology Liaoning. Her research interests focus on control theory and stability analysis of time-delay systems and multi-agent systems.

Liangdong Guo received the B.Sc. degree in Computational Mathematics and Applied Software and the M.Sc. degree in Operational Research and Cybernetics from the University of Science and Technology Liaoning (formerly Anshan Institute of Iron and Steel Technology), Anshan, China, in 2000 and 2005, respectively, and the Ph.D. degree in Control Theory and Control Engineering from Dalian University of Technology, Dalian, China, in 2011.

He is currently a Professor with the School of Sciences, University of Science and Technology Liaoning. His research interests include control theory, robust control, and the stability analysis of time-delay systems and multi-agent systems.

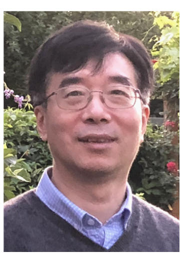

Zidong Wang (Fellow, IEEE) received the B.Sc. degree in mathematics from Suzhou University, Suzhou, China, in 1986, and the M.Sc. degree in applied mathematics and the Ph.D. degree in electrical engineering from Nanjing University of Science and Technology, Nanjing, China, in 1990 and 1994, respectively.

From 1990 to 2002, he held teaching and research appointments in universities in China, Germany, and the U.K. He is currently a Professor of Dynamical Systems and Computing with the Department of Computer Science, Brunel University of London, Uxbridge, U.K. He has authored number of papers in international journals. His research interests include dynamical systems, signal processing, bioinformatics, and control theory and applications.

Prof. Wang is a member of the Academia Europaea and the European Academy of Sciences and Arts, an Academician of the International Academy for Systems and Cybernetic Sciences, a fellow of the Royal Statistical Society, and a member of program committee for many international conferences. He holds of the Alexander von Humboldt Research Fellowship of Germany, the JSPS Research Fellowship of Japan, William Mong Visiting Research Fellowship of Hong Kong. He serves (or has served) as the Editor-in-Chief for *International Journal of Systems Science*, *Neurocomputing*, *Systems Science & Control Engineering*, and an Associate Editor for 12 international journals including *IEEE Transactions on Automatic Control*, *IEEE Transactions on Control Systems Technology*, *IEEE Transactions on Neural Networks*, *IEEE Transactions on Signal Processing, and IEEE Transactions on Systems, Man, and Cybernetics–Part C: Applications and Reviews*.

Lei Zou (Senior Member, IEEE) received the Ph.D degree in control science and engineering in 2016 from Harbin Institute of Technology, Harbin, China.

He is currently a Professor with the School of Information and Intelligent Science, Donghua University, Shanghai, China. From October 2013 to October 2015, he was a visiting Ph.D. student with the Department of Computer Science, Brunel University London, Uxbridge, U.K. His research interests include control and filtering of networked systems, moving-horizon estimation, state estimation subject to outliers, and secure state estimation.

Prof. Zou serves (or has served) as an Associate Editor for *Neurocomputing*, *International Journal of Systems Science*, *IEEE/CAA Journal of Automatica Sinica*, *IET Control Theory & Applications*, and *International Journal of Control, Automation and Systems*. He is a Senior Member of *IEEE* and *Chinese Association of Automation*, a Regular Reviewer of *Mathematical Reviews*, and a very active reviewer for many international journals.